

# Fluorescence, Scanning Electron Microscope (SEM), Non - Linear Optical (NLO) and Impedance of Swift heavy Ion ( $\text{Au}^{3+}$ ) Irradiated 2-Amino-5-Nitropyridinium Sulfamate (2A5NPS) Single Crystal

M. Ambrose Rajkumar<sup>1\*</sup>, Prof. Amjad Hassan Khan MK<sup>2</sup>, R. Aswin Herbert Sathish<sup>3</sup>, P. Ajith<sup>4</sup>, S. Pratap<sup>5</sup>, Prem Anand Devarajan<sup>4\*</sup>

1. Department of Physics, Kristu Jayanti College (Autonomous), Bengaluru-560077

2. Department of Electronics, Kristu Jayanti College (Autonomous), Bengaluru-560077

3. Department of Computer Science, Kristu Jayanti College (Autonomous), Bengaluru-560077

4. Department of Physics, St. Xavier's College (Autonomous), Palayamkottai, Tamilnadu-627002

5. Department of Physics, Loyola College (Autonomous), Chennai. Tamil Nadu – 600034

## Abstract:

*A semiorganic crystal of 2- amino-5-nitropyridinium sulfamate was grown from slow evaporation method. Bulk crystals of 2-amino-5-nitropyridinium sulfamate (2A5NPS) was grown using assembled temperature reduction (ATR) apparatus. The as grown crystal was irradiated using  $\text{Au}^{3+}$  metallic ion. Morphology of pristine and irradiated crystal was studied. Surface of irradiated crystals were damaged heavily and it decreased the degree of crystallinity. Nonlinear optical properties of as grown pristine and irradiated were determined using Kurtz powder technique. A nonlinear optical property of irradiated crystal has decreased. The decrease of second harmonic generation (SHG) is due to higher ion fluence, which almost affected the noncentro symmetric packing of the molecular crystal. Complex impedance was studied using Princeton Applied Research (2 channels) with frequency range 1Hz to 1MHz and the bulk resistance and grain boundary resistance were calculated.*

## Introduction:

Swift heavy ion (SHI) bombardment can induce irreversible change of structure and chemical composition within a small surrounding the ion track [1]. Ion beam techniques are employed as appropriate tool to change the physical properties of materials. Due to the formation of defects, a change in the refractive index is observed which is used for the fabrication of buried wave guide and chemical resistance is also reduced to a little extend [2-4]. Recent decades have witnessed the rapid development of methods for transmitting optical information. Integrated optical devices particularly those based on new types of optical materials playing an increasingly crucial role in this context [5- 7]. SHI capable of break molecular bonds and create damage to the single crystal [8- 13]. New structure of 2-amino-5-nitropyridinium sulfamate was solved and bulk crystal of 2-amino-5-nitropyridinium sulfamate was grown using assembled temperature method (ATR) and structural, optical, electrical, mechanical, thermal properties were already reported. New structure of 2-amino- 5-nitropyridinium hydrogen oxalate was also solved. Semiorganic crystals of 2-amino 5-nitropyridinium sulfamate, 2-amino-5-nitropyridinium hydrogen oxalate, 2-amino-5-nitropyridinium dihydrogen phosphate, 2-amino-5-nitropyridinium

Chloride and 2-amino-5-nitropyridinium nitrate were grown by using assembled temperature method and results were reported [14– 21]. A detailed study of structural and optical of  $\text{Au}^{3+}$  irradiated semiorganic crystals of 2-amino-5-nitropyridinium sulfamate were compared with pristine crystal and reported [22]. In this research article fluorescence, scanning electron microscope (SEM), non - linear optical and impedance of ion ( $\text{Au}^{3+}$ ) irradiated 2-amino-5-nitropyridinium sulfamate (2A5NPS) nonlinear optical (NLO) single crystal is reported.

## 2. Experimental procedure

### 2.1. Crystal growth

A semi organic crystal of 2- amino-5-nitropyridinium sulfamate was grown from slow evaporation method. Bulk crystals of 2-amino-5-nitropyridinium sulfamate (2A5NPS) was grown using assembled temperature reduction (ATR) apparatus. A good quality single crystal from slow evaporation used as a seed crystal for bulk growth  $5 \times 3 \times 2\text{mm}^3$  size of crystal was harvested after 60 days [23]. A cut and polished 2-amino-5-nitropyridinium sulfamate is shown in fig.1.

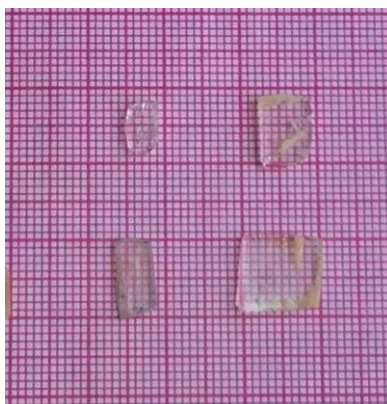


**Fig.1. Cut and polished 2-amino-5-nitropyridinium sulfamate (2A5NPS) NLO single crystal**

### 2.2. $\text{Au}^{3+}$ ion irradiation

A polished single crystal of 2-amino-5-nitropyridinium sulfamate(2A5NPS) from Assembled Temperature Reduction (ATR) method was used for irradiation. The grown crystals were irradiated in National Centre for Accelerator based Research (NCAR), Department of Pure & Applied Physics, Guru Ghasidas Vishwavidyalaya (Central University), at Bilaspur, Chhattisgarh using 3.0 MV Pelletron Tandem Accelerator. The polished crystalline samples were kept in a stainless steel sample holder. Copper paste was used to make contact between sample and holder. A source of negative ions by cesium sputtering (SNICS)  $\text{Au}^{3+}$  was selected for irradiation.  $\text{Au}^{3+}$  of 10.8 MeV with different fluences  $1 \times 10^{13}$ ,  $5 \times 10^{13}$  and  $1 \times 10^{14}$  ions/cm<sup>2</sup> with beam current of 1.55 $\mu\text{A}$ , 1.35  $\mu\text{A}$  and 8 PnA respectively was used for irradiation at room temperature. Ion beam

was magnetically scanned over a sample normal to its face for uniform irradiation. In this research work  $\text{Au}^{3+}$  ions of 10.8 MeV swift heavy ion (SHI) used for irradiation at room temperature.

### 3. Results and discussion

#### 3.1.1 Fluorescence study

Emission spectra of pristine and irradiated crystal of 2-amino-5-nitropyridinium sulfamate (2A5NPS) NLO single crystal are shown in Figure 3.11. Fluorescence spectra were measured at room temperature. It is observed from the fluorescence spectra that high peak intensity of pristine is 516 nm. Energy band gap of this high peak intensity was found to be 2.4 eV, using energy relation  $E_g = 1.24/\lambda$ . Emission of green light (516 nm) is due to  $\pi-\pi^*$  transition in the molecule. It is also absorbed that after irradiation the intensity of peak decreases and also there is a shifting of peak position when  $\text{Au}^{3+}$  ion increases from  $10^{13}$  to  $10^{14}$  ions/cm<sup>2</sup>. Peak intensity of ion fluence  $10^{13}$  ions/cm<sup>2</sup>,  $5 \times 10^{13}$  ion/cm<sup>2</sup> and  $10^{14}$  ions/cm<sup>2</sup> are 521 nm, 526 nm and 529 nm respectively. This decrease of intensity is due to lattice deformation and cation displacement. Defects are too many in higher fluence, which affects the radiation transition in single crystal and also acts as non radiative recombination centers. Irradiated 2-amino-5-nitropyridinium sulfamate (2A5NPS) NLO single crystal losses its luminescence property is due to large defects.

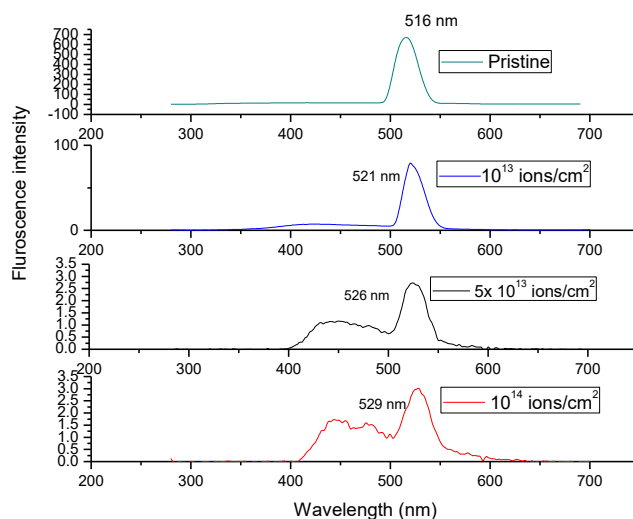


**Fig.3.11 Fluorescence spectra of pristine and  $\text{Au}^{3+}$  ion irradiated 2-amino-5-nitropyridinium sulfamate (2A5NPS) NLO single crystal.**

#### 3.2 Scanning electron microscopy (SEM)

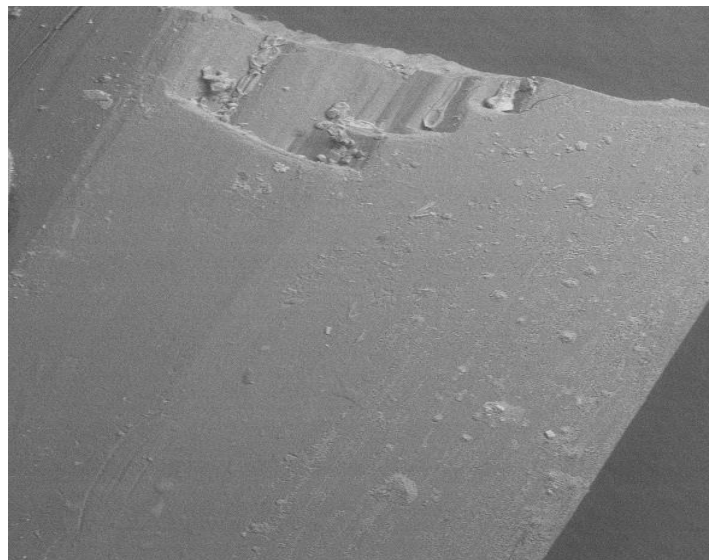


Fig. 3.21 SEM image of 2-amino-5-nitropyridinium sulfamate (2A5NPS) NLO single crystal.

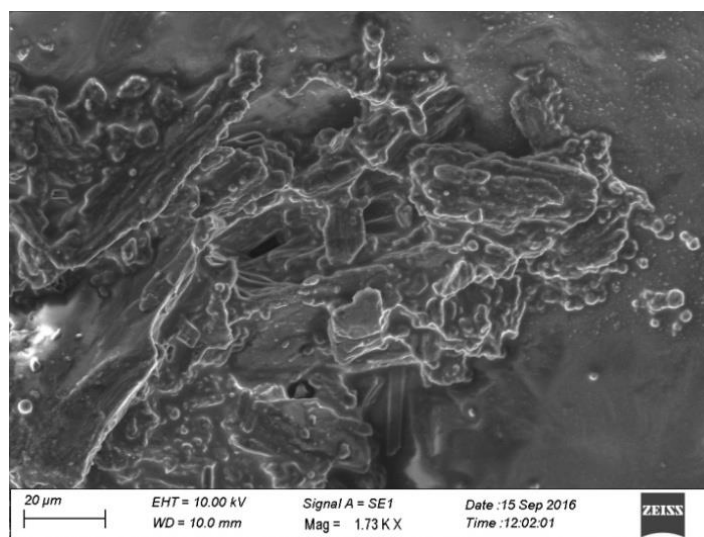
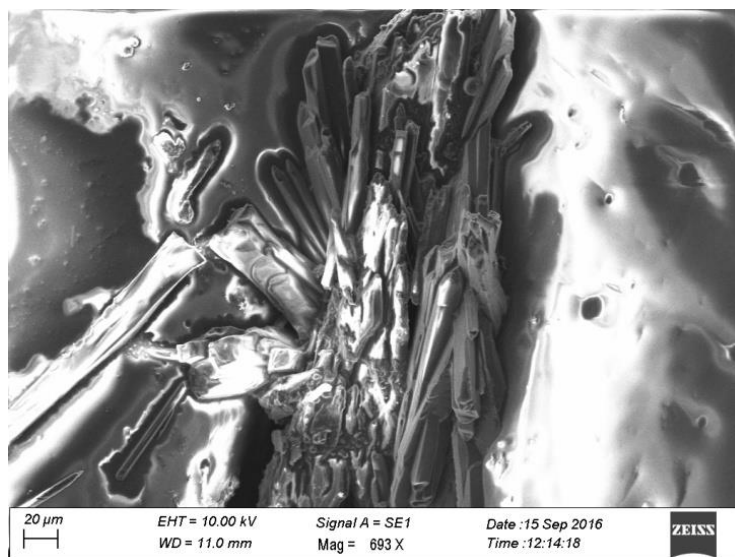
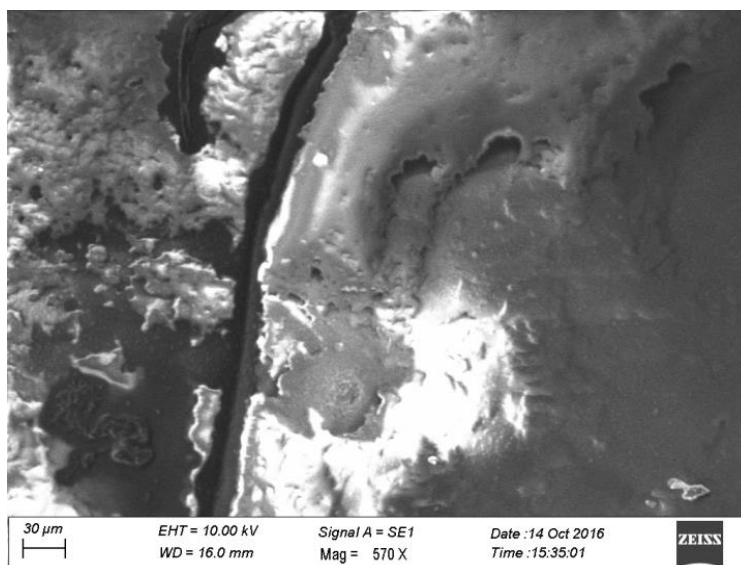


Fig. 3.22 SEM image of Au<sup>3+</sup> ion irradiated ( $10^{13}$  ions/cm<sup>2</sup>) 2-amino-5-nitropyridinium sulfamate (2A5NPS) NLO single crystal.



**Fig. 3.23 SEM image of Au<sup>3+</sup> ion irradiated ( $5 \times 10^{13}$  ions/cm<sup>2</sup>) 2-amino-5-nitropyridinium sulfamate (2A5NPS) NLO single crystal.**



**Fig. 3.23 SEM image of Au<sup>3+</sup> ion irradiated ( $10^{14}$  ions/cm<sup>2</sup>) 2-amino-5-nitropyridinium sulfamate (2A5NPS) NLO single crystal.**

The scanning electron microscopy (SEM) studies provide the information about topological features, morphology, phase distribution, compositional differences and crystal orientation. The SEM image of pristine and irradiated crystals of 2-amino-5-nitropyridinium sulfamate is shown in Figure 3.21, 3.22, and 3.23. The SEM image shows some morphological modification changes after irradiation and modified morphology exhibits in stepped structure at lower ion fluence. Variations in step directions and appearance of wider steps could be attributed

to the general roughness grain boundary caused by swift heavy ion (SHI). At higher fluences ( $5 \times 10^{13}$  and  $10^{14}$  ions/cm<sup>2</sup>) of Au<sup>3+</sup> vally like produced as the fluence increases along with ion tracks are also seen. Crystal surface was damaged heavily at higher fluence and also noticed that defects cluster were formed and they were isolated from each other, which confirms the increase of capacitance due to the Au<sup>3+</sup> irradiation. The accumulation of radiation damage with progressive structural degradation might lead to the decrease of crystallinity of the single crystal during the process of swift heavy ion irradiation. At lower fluence, defects are formed as cluster and on the fluence of SHI increases as defects formed on the surface increase [14].

### 3.3. NLO test

Nonlinear optical properties of as grown crystal were determined using Kurtz powder technique. A Q-pulsed Nd-YAG laser of 1064 nm was used as primary source and pulse width of 10 ns and repetition rate of 10Hz. Input of 1.2 mJ/ pulse laser was collimated on the sample using 20 cm focal of a convex lens via right angled prism. The sample was powdered and filled in a micro capillary tube. Output of second harmonic generation was seen on digital oscilloscope through monochromator and photomultiplier. Output of green laser of 534 nm was seen on oscilloscope. It is noticed from the result that SHG output for pristine sample was 24 mV and output of irradiated samples were 4 mV, 1mV, 1mV for ion fluence  $10^{13}$  ions/cm<sup>2</sup>,  $5 \times 10^{13}$  ions/cm<sup>2</sup> and  $10^{14}$  ions/cm<sup>2</sup> respectively whereas that of KDP was 22 mV. It is elucidated from the result that, when the samples are subjected to laser thermal diffusion which comes to play and damage the crystal further. Spreading of thermal energy increases along the swift heavy ion (SHI) path, defects in the crystal surface also increase as second harmonic generation (SHG) efficiency decreases. The decrease of second harmonic generation (SHG) is due to higher ion fluence, which almost affected the noncentro symmetric packing of the molecular crystal. Swift heavy ion (SHI) irradiated crystals are also rich in defects.

### 3.4. Impedance analysis

Impedance analysis is used to study electrical processes that are taking place within the crystalline sample and to characterize the bulk resistance of crystalline sample. Complex impedance was studied using Princeton Applied Research (2 channels) with frequency range 1Hz to 1MHz. The frequency dependent properties are represented in terms of complex impedance  $Z^* = Z' - j Z''$ , where  $z'$  and  $z''$  are real and imaginary part of impedance. Figure 3.41 and 3.42 shows frequency response real and imaginary part of impedance. It is understand from the graph that impedance decreases with increase of frequency. High value of impedance at lower frequency indicates that polarization is large. Debye-type dielectric dispersion is noticed in the frequency dependence curve (Banarji Behera et al 2007). It is observed from the real and imaginary impedance that the peak in the plots is relaxation process and peak frequency is equal to relaxation frequency. Relaxation process increases with increase of ion fluences. This is due to defects formation in the crystalline surface. It is also elucidated from the graph that the real and imaginary part of impedance decreases as frequency increases which indicates the increasing

conduction mechanism with applied frequency. Figure 3.43 shows Nyquist's plot of pristine and  $\text{Au}^{3+}$  ion irradiated 2-amino-5-nitropyridinium sulfamate (2A5NPS) NLO single crystal. A semicircle is seen in pristine and as well as  $\text{Au}^{3+}$  ion irradiated crystal due to bulk effect of the sample. A combination of capacitor and resistor creates bulk effect in the samples. It is also noticed from the Nyquist's plot that bulk resistance of irradiated crystal were increased more than the pristine crystal. It is also revealed from the graph that bulk resistance increases with increase of ion fluences from  $10^{13}$  ions/cm<sup>2</sup> to  $10^{14}$  ions/cm<sup>2</sup>. The bulk resistance and grain boundary resistance was calculated from the intercept of the semicircle arc on the real axis and peak of the semi circle respectively. Table.3.1 shows bulk resistance and grain boundary resistance of pristine and irradiated crystal.

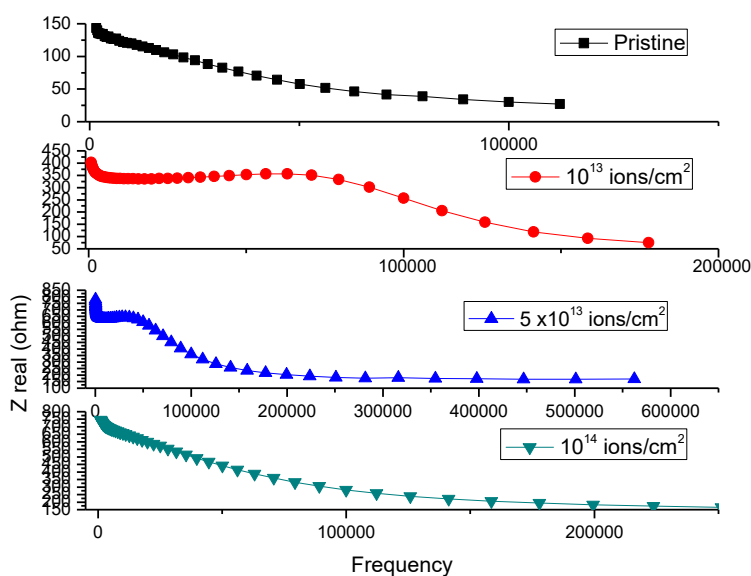


Fig. 3.41 Real part impedance of pristine and  $\text{Au}^{3+}$  ion irradiated 2-amino-5-nitropyridinium sulfamate (2A5NPS) NLO single crystal.

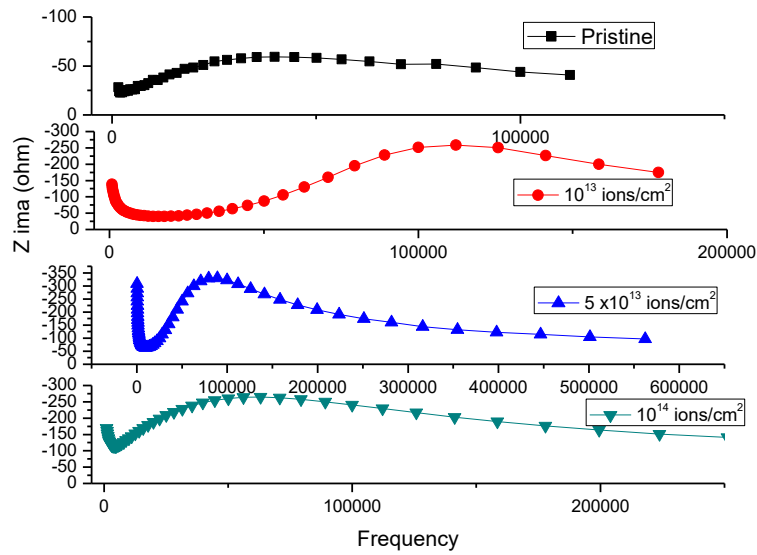


Fig. 3.42 Imaginary part of pristine and Au<sup>3+</sup> ion irradiated 2-amino-5-nitropyridinium sulfamate (2A5NPS) NLO single crystal.

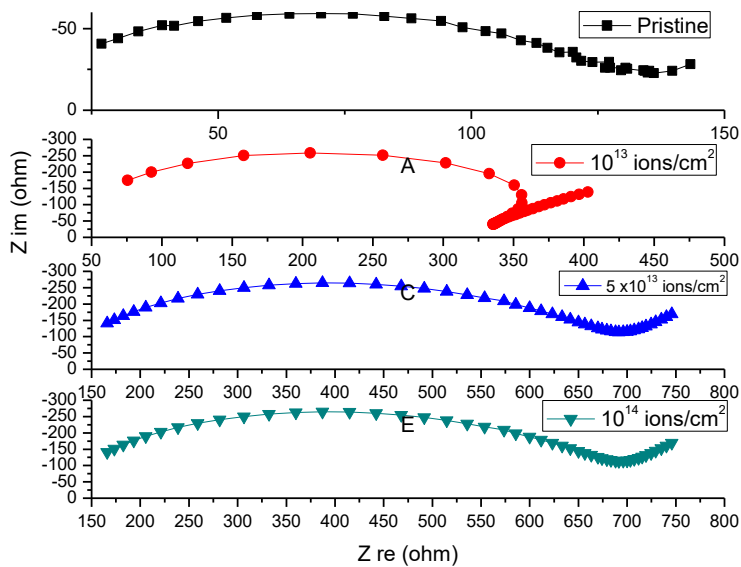


Fig. 3.43 Nyquist's plot of of pristine and Au<sup>3+</sup> ion irradiated 2-amino-5-nitropyridinium sulfamate (2A5NPS) NLO single crystal.

S.No	Ion fluence	Bulk resistance (Ohm)	Grain boundary resistance (Ohm)
1	Pristine	70.65	140
2	$10^{13}$ ions/cm <sup>2</sup>	208.21	285
3	$5 \times 10^{13}$ ions/cm <sup>2</sup>	403	670
4	$10^{14}$ ions/cm <sup>2</sup>	411.4	686

**Tab. 3.1 Bulk resistance and grain boundary resistance of pristine and Au<sup>3+</sup> ion irradiated 2-amino-5-nitropyridinium sulfamate (2A5NPS) NLO single crystal.**

### Conclusion:

A semiorganic crystal of 2- amino-5-nitropyridinium sulfamate was grown from slow evaporation method. Bulk crystals of 2-amino-5-nitropyridinium sulfamate (2A5NPS) was grown using assembled temperature reduction (ATR) apparatus. The as grown crystal was irradiated using Au<sup>3+</sup> metallic ion. Fluorescence was studied and it revealed that defects were rich in higher fluence, which affected the radiation transition in single crystal and also acts as a non-radioactive recombination centers. Morphology of pristine and irradiated crystal was studied and it was noted that surface of irradiated crystals were damaged heavily and it decreased the degree of crystallinity. The decrease of second harmonic generation (SHG) was due to higher ion fluence, which almost affected the noncentro symmetric packing of the molecular crystal. It was also elucidated from the impedance that the real and imaginary part of impedance decreased as frequency increased which indicated the increasing conduction mechanism with applied frequency.

### Reference

- [1]. Youmei Sun, Chonghong Zhang, Zhiyong Zhu, Zhiguang Wang, Yunfan Jin, Jie Liu, Ying Wang, The thermal-spike model description of the ion-irradiated polyimide, Nuclear Instruments and Methods in Physics Research Section B: Beam Interactions with Materials and Atoms, Volume 218, June 2004, Pages 318-322
- [2]. P.D. Townsend, P.J. Chandler, and L. Zhang, Optical effects of ion implantation, Cambridge Cambridge University Press - Cambridge studies in modern optics , 1994.
- [3]. J. Olivares, G. García, A. García-Navarro, F. Agulló-López, O. Caballero and A. García-Cabañes, Generation of high-confinement step-like optical waveguides in LiNbO3 by swift heavy ion-beam irradiation, Appl. Phys. Lett. 86, (2005), 183501.
- [4]. Feng Chen, Xue-Lin Wang, Ke-Ming Wang, Development of ion-implanted optical waveguides in optical materials: A review, Optical Materials 29 (2007) 1523–1542.

- [5]. Tie-Jun Wang, Yu-Fan Zhou, Xiao-Fei Yu, Tao Liu, Lian Zhang, Hong-Lian Song, Mei Qiao, Xue-Lin Wang, Optical waveguide properties of  $\text{Ca}_{0.4}\text{Ba}_{0.6}\text{Nb}_2\text{O}_6$  crystal formed by oxygen ion irradiation, Volume 354, 1 July 2015, 187-191
- [6]. T. Kanagasekarana, d, P. Mythilia, G. Bhagavannarayanab, D. Kanjilalc, R. Gopalakrishnana, , Investigations of structural, dielectric and optical properties on silicon ion irradiated glycine monophosphate single crystals, Nuclear Instruments and Methods in Physics Research Section B: Beam Interactions with Materials and Atoms, Volume 267, Issue 15, 1 August 2009, Pages 2495–2502
- [7]. V. Krishnakumar, D.K. Avasthi, Fouran Singh, P.K. Kulriya, R. Nagalakshmi, Study of the damage produced in  $\text{K}[\text{CS}(\text{NH}_2)_2]_4\text{Br}$  – A non-linear optical single crystal by swift heavy ion irradiation, Nuclear Instruments and Methods in Physics Research Section B: Beam Interactions with Materials and Atoms, Volume 256, Issue 2, March 2007, Pages 675-682
- [8]. H. Nagabhushana, S.C. Prashantha, B.M. Nagabhushana, B.N. Lakshminarasappa, Fouran Singh, Damage creation in swift heavy ion-irradiated calcite single crystals: Raman and Infrared study, Spectrochimica Acta Part A 71 (2008) 1070–1073).
- [9]. A. Deepthy, K.S.R.K. Rao, H.L. Bhat, R. Kumar, K.Asokan, Gray track formation in  $\text{KTiOPO}_4$  by swift ion irradiation, J .Appl .Phys .89 (2001) 6560.
- [10]. H. Nagabhushana , S.C. Prashantha, B.M. Nagabhushana, B.N. Lakshminarasappa, Fouran Singh, R.P.S. Chakradhar, Ion beam-induced luminescence and photoluminescence of 100 MeV  $\text{Si}^{8+}$  ion irradiated kyanite single crystals, Solid State Communications, Volume 147, Issues 9–10, September 2008, Pages 377–380.
- [11]. J. Olivares, A. García-Navarro, G. García, F. Agulló-López, F. Agulló-Rueda, A. García-Cabañes and M. Carrascosa, Buried amorphous layers by electronic excitation in ion-beam irradiated lithium niobate: Structure and kinetics, J. Appl. Phys. 101, 033512 (2007)
- [12]. Kanagasekaran, T., Gunasekaran, M., Srinivasan, P., Jayaraman, D., Gopalakrishnan, R. and Ramasamy, P., Studies on Growth, Induction Period, Interfacial Energy and Metastable Zone Width of m-Nitroaniline. Crystal Re-search and Technology, 40, (2005),1128-1133
- [13]. I.P. Jain, Garima Agarwal, Ion beam induced surface and interface engineering, Surface Science Reports, 66, Issues 3–4, March 2011, Pages 77–172.
- [14]. K. Suriya kumar, S. Gokul Raj, G.Ramesh Kumar and R. Mohan, 50Mev  $\text{Li}^{3+}$  irradiation effects on structural, optical and surface properties of L- Alanine single crystal, Science of advanced materials, vol.1, 2009, 286-291.

[15]. M. Ambrose Rajkumar, X. Stanly John Xavier, S. Anbarasu, D. Prem Anand, 2- Amino-5-nitropyridinium sulfamate, Acta Cryst. (2015). E71

[16]. M. Ambrose Rajkumar, X. Stanly John Xavier, S. Anbarasu, D. Prem Anand, 2- Amino-5-nitropyridinium hydrogen oxalate, Acta Cryst. (2014). E70, o473–o474

[17]. M. Ambrose Rajkumar, S.Stanly John Xavier, S.Anbarasu, D. Prem Anand, Microhardness, Dielectric and Photoconductivity Studies of 2-Amino-5-nitropyridinium hydrogen oxalate Single Crystal, International Journal of Emerging Trends in Science and Technology Vol.10, P.1579 1585 (2014).

[18]. M. Ambrose Rajkumar, S.Stanly John Xavier, S.Anbarasu, D. Prem Anand, Microhardness, Dielectric and Photoconductivity Studies of 2-Amino-5-nitropyridinium dihydrogen phosphate Single, Crystal, International Journal of Emerging Trends in Science and Technology Vol.10, P.1579-1585 (2014).

[19]. M. Ambrose Rajkumar, S.Stanly John Xavier, S.Anbarasu, D. Prem Anand, Growth and characterization studies of an efficient semiorganic NLO single crystal: 2-Amino-5-nitropyridinium sulfamate (2A5NPS) by assembled temperature reduction (ATR) method, Optical Materials 55 (2016) 153–159.

[20]. M. Ambrose Rajkumar, S.Stanly John Xavier, S.Anbarasu, D. Prem Anand, A Convenient Route to Synthesize and Grow 2-Amino-5-Nitro Pyridinium Nitrate Crystals for Laser generation, Scientia Acta Xaveriana 4(2), (2014) 73-78.

[21]. M. Ambrose Rajkumar, S.Stanly John Xavier, S.Anbarasu, D. Prem Anand, Microhardness, Dielectric and Photoconductivity studies of 2- Amino-5- Nitro Pyridinium Nitrate NLO Single crystals, Res. J. Physical Sci., 2(1),1-4(2014).

[22]. M. Ambrose Rajkumar, A. Ajeeth, S. Anbarasu, Prem Anand Devarajan, Irradiation effect of Au<sup>3+</sup> on 2-amino-5-nitropyridinium sulfamate (2A5NPS) NLO single crystal, AIP Conference Proceedings, 2270, 100002-1–100002-6

[23]. M. Ambrose Rajkumar, S.Stanly John Xavier, S.Anbarasu, D. Prem Anand, Growth and characterization studies of an efficient semiorganic NLO single crystal: 2-Amino-5-nitropyridinium dihydrogen phosphate (2A5NPDP) by Sankaranarayanan-Ramasamy (S-R) method, Optik 127, 2187-2192 (2016).